DETERMINATION OF INTERNAL TEMPERATURE PROFILES BY MULTIFREQUENCY RADIOTHERMOGRAPHY IN MEDICAL APPLICATIONS

K. P. Gaikovich, M. I. Sumin,
and R. V. Troitskii

UDC 621.371f615.47

Results are presented from theoretical and experimental studies of a method for determining temperature stratification of body tissues using multifrequency measurements of the body's thermal radio radiation. The corresponding converse problem is solved for media with multilayer dielectric structure, and numerical experiments are performed, on the basis of which the capabilities of the method are determined and requirements formulated for frequency ranges and necessary measurement accuracy. Data of three-channel measurements at wavelengths of 9, 30, and 60 cm are used to reconstruct temperature profiles in tissues containing tumors. The method is used to monitor the intensity and localization of tissue heating during tumor treatment by uhf hyperthermy.

At present there is great interest in the possibility of reconstructing temperature profiles over depth in biological media, in particular, in the human body, from measurements of thermal radio radiation produced by such media. The thickness of the layer in which the thermal radiation is formed depends on the wavelength, varying from a fraction of a millimeter to several centimeters, which in principle permits use of radio radiation spectra to reconstruct temperature distribution down to depths of several centimeters. Determination of interior body temperature significantly expands diagnostic possibilities as compared to measurements in the IR range, which allow temperature measurement only on the skin surface. The objects of study might be inflammatory or timorous processes, or other disease processes which produce a local temperature elevation within the; depths of tissues. The value of such remote noninvasive measurements is obvious when the difficulties of direct measurements involving insertion of a sensor into the body are considered. An important advantage of radiometric methods is' their ability to provide data continuously on a real tine basis. One possible concrete application, having great practical significance, would be monitoring the amount and localization of heating during treatment of tumors by uhf hyperthermy, i.e., heating by high power uhf radiation.

Methods of long distance thermal probing, first, developed in radio astronomy, have been elaborated to a great extent in studies of the height profile of temperature in the atmosphere (1, 2). However, direct use of this accumulated experience for reconstructing temperature profiles in biological media is difficult. These difficulties involve foremost the specifics of the medium in question, namely its multilayer structure, which causes re-reflections between layers and interference of the radiation, as well as intense absorption in tissues, which makes use of the concept of ray intensity inapplicable- in such a medium [3].

The results of th« present study rely on investigations reported in a number of previous studies. Dielectric parameters of various tissues were calculated using the data of [4]. Significant achievements in developing methods for solution of this type of converse problem wore presented in [5, 6]. Those studies developed and successfu1ly applied a method for reconstructing temperature profiles based on the ideas of solving incorrect converse problems formulated by Tikhonov's mathematical school [7, 8]. At present a solution has been obtained for thermal radiation from a half-space with multilayer dielectric structure for both a three-layer model (see, for example, [9-]), and in the general case, in particu-

Scientific-Research Institute of Radiophysics. Translated from Izvestiya Vysshih Uchebnikh Zavedenii, Radiofizika, Vol. 31. No. 9, pp. 1104-1112, September, 1988. Original article submitted August 20, 1986.

 0033-8443/88/3108-0786$12.50

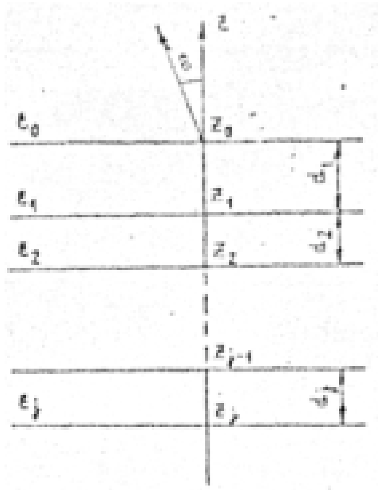

Fig. 1. Half-space with layered dielectric structure. The quantity ε_j is constant within each layer, while temperature is a continuous function.

lar, in [10], where the relationship of brightness temperatures to the temperature profile was expressed by a Fredholm integral equation of the first kind, allowing use, of solution methods developed in (6).

Significant progress has also been achieved in the area of experimental studies. A radiometric apparatus has been developed with special contact antennas, a method for reflection compensation by noise introduction has been tested, model estimates of temperature profiles have been performed using data from one-channel measurements (11, 12], and calibration errors in brightness temperature measurements have been considered [13).

1. Thermal Radiation of a Multilayer Medium. Formulation of Converse Problem.

We will consider the thermal radio radiation of a half-space with multilaver structure having a complex dielectric permittivity $\varepsilon=\varepsilon'-i\varepsilon''$, following (10) (Fig.1). Solution of the electrodynamic problem for such a structure allows use of the electric field coherence function at the boundary z = 0 to calculate the intensity of thermal radio radiation and its brightness temperature in the form

$$T_B(\lambda) = \int_{-\infty}^{0} T(z)\, B(\lambda, z)\, dz\,, \tag{1}$$

where λ is the wavelength for layer j

$$B(\lambda, z) = \frac{B_j}{2}\left[\mathrm{Re}\,(k_j y_j)\left|e^{k_j(z-z_j)} + \Gamma_j e^{-k_j(z-z_j)}\right|^2 + \mathrm{Re}\,(k_j y_j^*)\left|e^{k_j(z-z_j)} - \Gamma_j e^{-k_j(z-z_j)}\right|^2\right], \tag{2}$$

while $z_N=z_{N-1}$.

The coefficients B_j are determined recursively beginning with $B_0 = 2/y_0$ by the expres-

$$B_j = B_{j-1}\frac{|1-\gamma_{j-1}|^2}{|e^{k_j d_j} + \gamma_{j-1}\Gamma_j e^{-k_j d_j}|^2} \quad (j = 1, 2, \ldots, N-1),$$

$$B_N = B_{N-1}|1+\gamma_{N-1}|^2,$$

where

$$\Gamma_j = \gamma_j + \frac{\Gamma_{j+1}\exp(-2k_{j+1}d_{j+1})}{1+\gamma_j\Gamma_{j+1}\exp(-2k_{j+1}d_{j+1})} \quad (j = 0, 1, \ldots, N-1),$$

$$\Gamma_N = 0, \quad k_j = \frac{2\pi}{\lambda}\sqrt{\varepsilon_0\sin^2\theta - \varepsilon_j},$$

$$\gamma_j = \frac{y_j - y_{j+1}}{y_j - y_{j+1}}, \quad \mathrm{Im}\,(k_j) < 0,$$

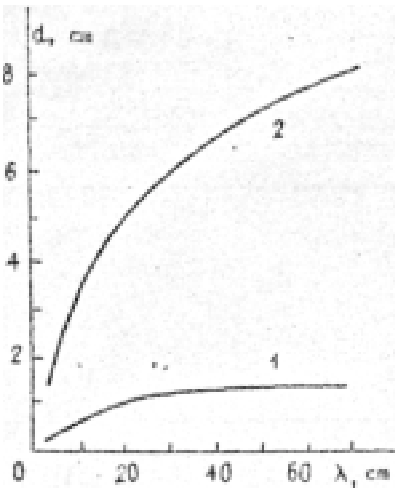

Fig. 2. Skin layer thickness vs wavelength:
1)muscle; 2) fat.

$$y_j = \begin{cases} \dfrac{k_j \lambda}{2\pi i c \mu^0} & \text{— for horizontal polarization,} \\[2ex] \dfrac{k_j \lambda}{2\pi i c \varepsilon^0 \varepsilon_j} & \text{— for vertical polarization.} \end{cases}$$

Here c is the speed of light and ε_0, μ_0 are the electric and magnetic constants, respectively.

The half-space reflection coefficient is defined by '

$$R = |\Gamma_0|^2 . \tag{3}$$

However, direct use of brightness temperature measurements is complicated, since it is difficult to perform absolute brightness temperature measurements to the required accuracy ($\delta T_B \leq$ 0.1 K.) because of uncertainty in the reflection coefficients *R*, which is caused by the lack of sufficient study of dielectric properties of biological media, including their temperature dependence (4).

These difficulties can be overcome successfully by using the method of noise introduction to compensate the effect of reflection. At a noise introduction temperature close to the temperature of the medium under study, the effect of reflection can be compensated almost completely and calibration error is determined by the accuracies to which the reference temperatures and compensation signal temperature T_n are known. With noise introduction the measured brightness temperatures satisfy the equation

$$T_B(\lambda) = \int_{-\infty}^{0} T(z)\, A(\lambda,z)\, dz + R\left(T_n - \int_{-\infty}^{0} T(z)\, A(\lambda,z)\, dz\right) , \tag{4}$$

where $A(\lambda,z)=B(\lambda,z)/(1 - R)$. Knowing the noise temperature T_n and relying on the smallness of the second term in Fq. (4), the T_B values can be used to determine the integral temperature of the medium

$$T_I(\lambda) = \int_{-\infty}^{0} T(z)\, A(\lambda,z)\, dz \tag{5}$$

to a high degree of accuracy, even if the constant *R* is known only a large uncertainty (~20%). In contrast to Eq. (1), for $T(z)$ = const = T_0, $T_I(\lambda) = T_0$, which indicates the independence of Eq. (5) from the reflection coefficient.

2 . Soluion of the Converse Problem. Numerica1 Experiment. Equation (5) is an incorrectly formulated problem in the sense of [7]. Its solution requires use of significant *a proori* information on the unknown exact solution. We have used Tikhonov's regularization method [7, 8] in the form of the generalized discrepancy principle, which utilizes quite general a priory information on the smoothness of exact solution. For compactness we write Eq.(5) in the form

$$AT = T_I^\delta , \quad AT \equiv \int_{-\infty}^{0} T(z)\, A(\lambda,z)\, dz . \tag{6}$$

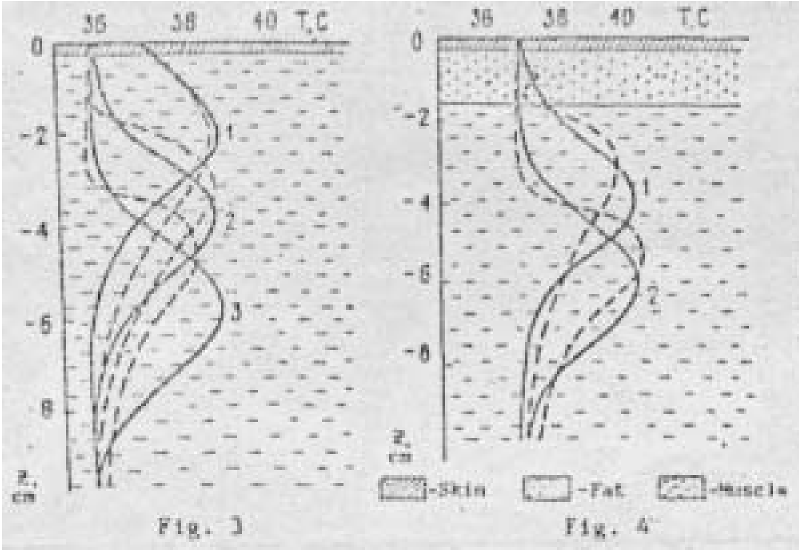

Fig. 3. Numerical modeling. Solid curves, original temperature profiles in the form of Eq. (9) with characteristic thickness Δz=2 cm, amplitude ΔT = 2 K and depths of maximum z_m =–2 cm (curve 1), z_m = -4 cm (curve 2), z_m = –6 cm (curve 3). Dashes, reconstructed profiler, δT_I = 0.1 K.

Fig.4. Numerical modeling. Solid curves, original profiles, depths of maxima z_m = -4 cm (curve 1), z_m = -6 cm (curve 2), Δz=2 cm , ΔT = 2 K. Dashes, reconstructed profiles with δT_I = 0.1 K.

where a > 0 is a sufficiently large number, T_I^δ is the measured realization of the right side, while

$$\int_c^d [\bar{T}_I(\lambda) - T_I^\delta(\lambda)]^2 \, d\lambda \leqslant \delta^2, \qquad d > c > 0,$$

$T_I(\lambda)$ is the right side of Eq. (4) corresponding to the exact solution $T(z)$, and δ^2 is the uncertainty of the measurement. According to [7, 8] to find the approximate solution of Eq. (6), and therefore, Eq. (5), it is necessary to minimize within the space W_2^1 (a, b) or the functions $T(x)$ (W_2^1 is the space of functions summable with a square on (a, b) which also have on (a, b) the generalized derivatives also summable with a square (for further detail see [14]) the functional

$$M^\alpha(T) = \|AT - T_I^\delta\|^2 + \alpha(\|T\|^2 + \|\frac{dT}{dz}\|^2), \tag{7}$$

where $\|X\|$ implies the norm of the function X as an element of the space of the functions summable with a square on the corresponding segment (determination of the norm in the space L_2 of functions summable with a square is described, for example, in [7], p. 35). For the regularization parameter α we choose here a nonnegative number which is a root of the one-dimensional nonlinear generalized discrepancy equation

$$\rho(\alpha) = \|AT^\alpha - T_I^\delta\| - \delta^2 = 0, \tag{8}$$

where T^α is the function which minimizes functional (7). We note that within the framework of the method of regularizing Fqs. (7), (8) we can easily consider *a priori* information on the nonnegativaness of the exact function. To do this the minimization of functional (7) must be carried out only on the set of nonnegative generally dlfferentiable functions $T(z)$. And in turn one can reduce to the case in which such important *a priori* information is known as that the unknown exact solution is without doubt larger (or without doubt smaller) for all $z\in[-a,0]$ than some *a priori* specified function. After the corresponding discretization the problem of minimization of functional (7) indicated above lead to finite-difference analog, which have been well studied from calculation viewpoint of the quadratic programming problem [15].

It should be noted that in the given case, in contrast to the problems considered in [1, 2, 5, 6] the integrand $A(\lambda,z)$ of the integral equation suffers discontinuities of the first kind at the points z_j, where the boundaries of the biological tissue layers with differing dielectric properties are located (skin-fat-muscle). Nevertheless, the formalism of the regularization method in the form of the generalized discrepancy principle can be applied in the case of integrand discontinuities, since the operator A defined by the integrand $A(\lambda,z)$ is in this case too a linear finite operator, acting from the space W_2^1 into the space $L_2(c, d)$.

As is well known [1, 2, 5, 6] in solving an incorrect problem the efficiency of a concrete- algorithm can be established only by numerical experiment. On the basis of the method presented above algorithms were developed for solution of Eq.(5) and numerical experiments were performed which permitted determination of the informative wavelength range, as well as requirements for accuracy levels and number of frequency channels needed for various $T(z)$ distributions having differing complexities, characteristic thicknesses, and temperature changes. The numerical experiments were performed in the following manner. Values of T_I for various wavelength were calculated for model $T(z)$ profiles. A normally distributed error with zero mean and specified dispersion was superposed on these values using a random number generator. The integral temperature measurements obtained in this manner were then used for solution of the converse problem. The accuracy of converse problem solution was evaluated by comparing the reconstructed temperature profile with the original $T(z)$ profile.

The numerical experiments showed that the basic types of $T(z)$ profiles could be reconstructed with good accuracy at measurement accuracies of δT_I = 0.01-0.03 K and approximately 10 channels in the informative centimeter and decimeter wavelength range. However, profiles with a relatively simple (for example, monotonic) structure were reconstructed fairly well with minimum measurement accuracy requirements ($\delta T_I \sim 0.1$ K) and 3-4 channels. The measurement wavelengths should be chosen such that the thickness of the skin laver increases uniformly from several millimeters to maximum values, since, the probing depth is determined by the skin-layer thickness ($d = \lambda / 4\pi \,\mathrm{Im}\sqrt{\varepsilon}$) [6]) of the probed tissues, which depends mainly on the water content in the tissues. For the basic tissue types the dependence of skin layer thickness on λ lies between the curves shown in Fig.2. We will note that the skin layer thickness of water varies with change in salinity within practically the same limits [6]. Qualitatively the solutions do not depend too greatly on choice of concrete wavelengths, in particular, one set which satisfies the conditions formulated would be λ_i = 2, 10, 30, 60 cm.

Results of the numerical modeling for a wavelength set λ_i = 9, 30, 60 cm (the same set used in our clinical experiments) are shown in Figs.3-6. The temperature distributions within the tissues were specified as a Gaussian profile

$$T(z) = T_0 + \Delta T \exp\left[-\left(\frac{z - z_m}{\Delta z}\right)^2\right].$$

Figure 3 shows a reconstruction of $T(z)$ profiles in muscle tissues. In solving the converse problem the limitation $T(z) \geq T_0$ was used, with the error level modeled being δT_I = 0.1 K. It is evident that for the given error level the form of the profile and the position of the maximum are well retrieved up to the depth of ≈ 4 cm. For further increase in depth the accuracy of the reconstruction decreases, since the contribution of deep layers to the radio emission decreases rapidly.

As follows from fig.2, a fat layer is more transparent to radiation, and its presence (see Fig.4) does not hinder reconstruction of the temperature profile in a tissue layer located deeper beneath it. The accuracy of reconstruction at depth of 6-8 cm increases (compare reconstructed curve 3 of Fig.3 with analogous curve of Fig.4).

Figure 5 is an example of reconstruction of a monotonic temperature distribution (z_m in Eq. (9) equal to zero).

It should be noted that with increase in the level of measurement error the accuracy of the reconstruction falls rapidly as is illustrated by the results shown in Fig.6. Of basic significance here is not the constant error component, which, as a rule, produces only

*****For the definition of linear finite operator in normalized spaces, see, for example, [14].

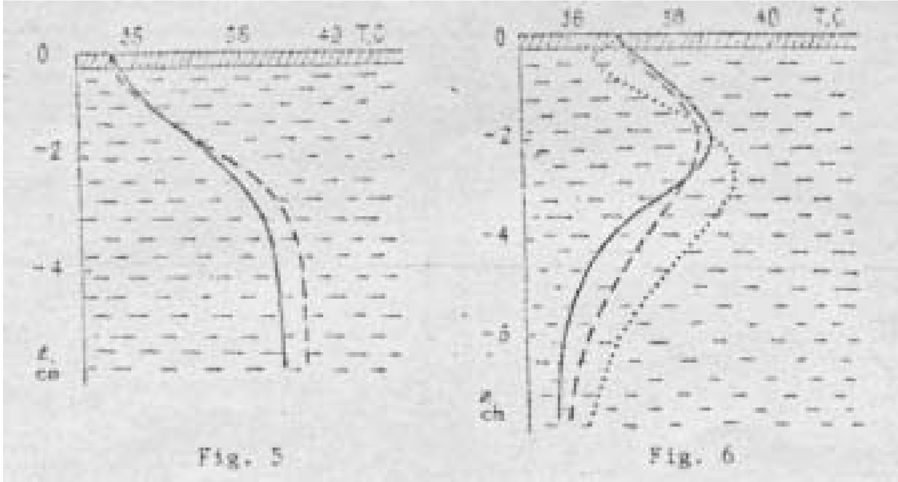

Fig. 5. Numerical modeling. Reconstruction of monotonic temperature profile (in Eq.(9) z_m=0, Δz=2 cm, ΔT= -2 K. Original profile, solid curve; dashes, reconstructions with δT_I = 0.1 K.

Fig. 6. Numerical modeling. Dependence of solution on error level modeled. Original profile, solid curve; dashes, reconstruction for δT_I = 0.1 K; dots, reconstruction for δT_I = 0.3 K.

a general shift of the reconstructed profile, but the random component, which destroys the relationship between the integral temperatures at different frequencies.

Of special importance is the role of a priori information in the form of limitations used in solving the converse problem It proves to be the case that one-sided limitation also eliminates significant deviations of the solution in the direction opposite the limitation, since these deviations cannot be compensated in the integral by deviations to the side where the limitation acts. Although the solution is not very critical with respect to the function limiting it from above or below, more precise specification of this function allows distinction of the informative part of the integral in Eq.(5), and the quality of the solution increases. We must stress that without use of limitations at realizable measurement accuracies it is impossible to solve the converse problem by this method to useful accuracy. In connection with this it would be desirable to develop maps of standard temperature distributions of human body together with maximum deviations from these distributions for various pathologies. In specifying limitations it is also possible to use surface temperature measurements and invasive internal point measurements within tissues.

High measurement accuracy can be achieved by measuring contrasts in integral temperatures in symmetric or closely situated body areas. In this case use of the unperturbed temperature profile of the healthy tissue as the limitation can be effective in determining the profile of the disturbance generated by the pathological process.

It follows from the calculations that for tissue dielectric parameters accuracies of approximately 10% are possible in solving the converse problem. The uncertainties in determining layer thickness should be much less than the wavelengths within the tissues.

3. Reconstruction of Temperature Profile from Clinical Measurement Data. Experimental studies were carried out in the Radiophysical laboratory of an oncology clinic. A radiometric system including three radiometric detectors at wavelengths of 9, 30, and 60 cm was used. The fluctuation threshold of radiometric sensitivity was not more than 0.05 K for a time constant of 1 sec. The measurements were carries out with the technique described in [14]. The compensation signal had a temperature T_n = 37±0.2 K, differing from the measured temperatures by not more than 3-4 K. In the calibration process radiation from salt water at constant temperatures close to those to be measures was used as a reference. The calibration data indicated that the uncertainty of the integral temperature measurements was no more than 0.15 K.

Figure 7 shows reconstructions of temperature profiles obtained by the radiometric method in the presence of tumor processes. Contact temperature measurements were made simultaneously

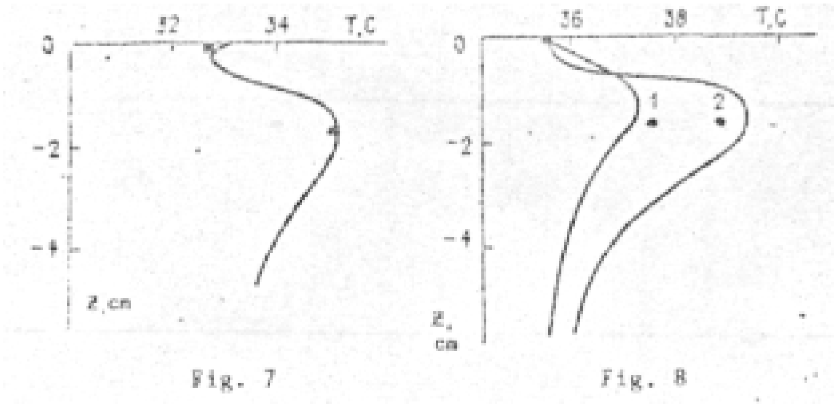

Fig. 7. Results of reconstruction by experimental three-channel measurements. Patient Sh. Tissue structure: skin, 1 mm; below: mammary gland (fat, connective tissue) with tumor. Solid curves, reconstructed $T(z)$ profile; circles, contact measurements.

Fig. 8. Temperature profile T(z) reconstructions from radiometric data before (curve l) and after (curve 2) uhf hyperthermy session. Patient S. Tissue structure: skin, 1 mm, tumor 1 cm, muscle. Circles, contact measurement data.

on the skin surface and at a depth of 1.5 cm using a needle sensor. The converse problem solution employed the natural limitation $T(z) \geq T(0)$ and it was assumed that the dielectric parameters of the tumor coincided with the corresponding parameters of the surrounding tissues.

For the case presented in Fig.7 the maximum temperature indicated bv the reconstruction results was 35.2° C at a depth of 1.5 cm, which practically coincided with the direct measurement data. Qualitative one can also judge the elevation of the internal temperature in the tumor directly from the integral temperature measurements. Thus, for a surface temperature of T_0 = 32.6 ^{0}C the integral temperatures were 33.5, 34.6, and 34.3 ^{0}C at wavelengths of 9, 30, and 60 cm, respectively. The results presented indicate the possibility of diagnostic study and monitoring tumor and inflammatory processes which lead to local temperature changes.

Another important application of radiometric probing could be monitoring the degree of tissue heating in tumor treatment by uhf hyprthermy. Temperature profile reconstructions before and after irradiation of tumor are presented in Fig.8. The tumor was irradiated by a hyperthrmy system operating at 915 MHz with power output 100 W. The skin surface was cooled by circulating water at constant temperatures so that the tissue temperature increases several degrees as the result of radiation. The slight temperature elevation before the hyperthermy was carried out is related to processes occurring in the tumor. The results presented indicate the good agreement of the reconstructed temperature values with contact measurement data at depth of 1.5 cm.

Thus the results obtained indicate the real promise as well as the limitations of the radiometric probing method for determining the temperature distribution over depth of a body by multifrequency measurements of thermal radio emission. In addition the results provide a methodological and algorithmic base for solving similar problems of probing other media with multiplayer dielectric structure. Progress in studies in this field will be related both to improvement in radiometric equipment and calibration methods to achieve higher measurement accuracy, and to further development of ever more precise methods and algorithms for solution of the converse problem with consideration of all available *a priori* information. As the numerical experiments show, the accuracy of reconstruction can be improved by increasing the number of measurement channels. In particular, inclusion of a channel with wavelength of 2-3 cm which provides information on tissue layers close to the surface is useful (Fig.2). The dielectric parameter values of various tissues must be refined and maps of body temperature distribution created. Solution of these problems could provide a new noninvasive instrument for diagnostics and monitoring of illnesses involving lical temperature changes within body tissues.

LITERATURE CITED

1. K. P. Gaikovioh et al., Int. J. Remote Sensing, 4, No. 2, 419 (1983).
2. H. R. Westwater et al., J. Climate Meteorology, 23, No. 5, 689 (1984).
3. L. A. Apresvan and Yu. A. Kravtsov, Theory of Radiation Transport [in Russian], Nauka, Moscow (1983). ;
4. Guy Johnson, Proc. IEEE, 60, No. 6 (1972).
5. N. A. Vaili'iiko, K. P. Gaikovich, and M. I. Sumin. Dokl. Akad. Nauk.SSSR, 290, No. 6, 1232 (1986) .
6. K. P. Gaikovich, A. N. Keznik, M. I. Sumin, and R. V. Troitskii , Preprint NIRFI No.214 [in Russian, Gor'kii (1986).
7. A. N. TikhouoY ami V. Ya . Arsenin. Methods for Solution of Incorrect Problems [in Russian], Nauka, Moscow (1979).
8. A. N. Tikhonov, A. V. Goncharskii, V. V. Stepanov, and A. G . Yagola, Regularizing Algorithms and A priori Information [in Russian], Nauka, Moscow (1983).
9. F. Bardati and D. Solimini, Radio Sci., GE-22 No. 4, 374 (1983).
10. F. Bardati and D. Solimini, IEEE Trans. GE-22 No. 4, 374 (1984).
11. V. S. Troitskii, V. A. Aranzhereev, A. V. Custov. et al., Izv. Vyssh. Ucheb. Zaved., Radiofiz., 29, No. 1, 62 (1986).
12. V. S. Troitskii, V. I. Abranov, I. F. Belov, et al., Izv. Vyssh. Ucheb. Zaved., Rariiofiz., 24_, No. 1 , 118 (1981).
13. L. S. Pavlova and V. M. Polvakov, Collected Studies of the All-Union Conference on Methodological Questions in Determination od Temperature of Biological Speciments by Radiophysical Methods [in Russian] , IRE Akad. Nauk SSSR, Moscov (1985), p. 8.
14. V. I. Smirnov, Course in Higher Mathematics, Vol. 5 [in Russian], Fizmatgiz, Moscow (1959).
15. F. L. Vasil'ev, Numerical Methods for Solution of Extremal Problems (In Russian], Nauka, Moscow (1980).